

A cold-atoms based processor for deterministic quantum computation with one qubit in intractably large Hilbert spaces

C. W. Mansell¹ and S. Bergamini¹

¹*The Open University, Walton Hall, Milton Keynes, MK7 6AA*

(Dated: February 26, 2022)

We propose the use of Rydberg interactions and ensembles of cold atoms in mixed state for the implementation of a protocol for deterministic quantum computation with one quantum bit (DQC1) that can be readily operated in high dimensional Hilbert spaces. We propose an experimental test for the scalability of the protocol and to study the physics of discord. Furthermore we develop a scheme to add control to non-trivial unitaries that will enable the study of many-body physics with ensembles in mixed states.

I. INTRODUCTION

At present, no single feature of the quantum world has been identified as the source of the computational enhancement, efficiency and speed-up of quantum protocols. Whilst entanglement is widely recognised as a key resource in quantum technology [1], an exponential advantage over classical computing can be achieved without it [2] in the presence of non-classical correlations (discord). Experiments using few photonic qubits [3] have shown that some computational tasks that are classically intractable can be efficiently solved even with no entanglement. The dynamics of entanglement and discord differ considerably, with entanglement being extremely fragile towards decoherence (even undergoing entanglement sudden death [4]) and discord being much more robust [1]. Since decoherence is a major hurdle to the development of quantum technologies [5, 6], the investigation of protocols that are more robust against it is a promising route for progressing the field.

In the past years, there has been outstanding progress in the demonstration of quantum algorithms based on pure states with a limited number of qubits. However scalability remains an issue, mainly because of decoherence. In pure-states quantum computation (QC) this problem can possibly be solved by error correction. Nevertheless, scaling up to a significant number of qubits and being able to perform a classically intractable calculation has been impossible so far.

Deterministic quantum computation with one qubit (DQC1) is a non-universal model based on mixed states that can exponentially speed up some computational tasks for which no efficient classical algorithms are known. DQC1 protocols present a remarkable advantage with respect to standard QC protocols, in that it requires only a single qubit with coherence to perform large scale quantum computation, whilst its power scales up with a number of qubits in mixed state. It is therefore in principle more readily scalable, provided a suitable system for the implementation is developed. Although it has been shown that this scheme contains little to no entanglement [7], non-classical correlations are present in the output state of the DQC1 which can be quantified in terms of quantum discord [8]. Discord has been

shown to be a valuable resource for specific computational tasks and for being extremely robust towards decoherence [5], which is the stumbling block in developing quantum technologies [9], [1]. To date, successful experiments based on DQC1 have evaluated the normalised trace of a two-by-two unitary matrix [3] and performed the approximation to the Jones polynomial with a system of four qubits [10], thus demonstrating the ground principle of mixed state computation. However, these experiments were performed with photons and nuclear magnetic resonance respectively, with limited scalability so far. Eventually, like for pure states quantum computation, the protocol is useful only if it can be scaled up and run over a significant number of qubits. Therefore DQC1 needs to be tested and operated in large Hilbert spaces, so it is vital to benchmark it in a system that allows to reach this regime.

We propose a new scheme to investigate experimentally the physics of DQC1 and discord in many-atom ensembles for a specific algorithm that performs the normalized trace estimation [11]. Cold ensembles in micron-sized dipole traps can contain a few to hundreds of atoms and we find that the protocol under study is robust enough to be operated both in small and large ensembles. We demonstrate that applying the protocol on an ensemble of 100 atoms will successfully evaluate the normalized trace of a 2^{100} -by- 2^{100} matrix. Finding the normalised trace of this matrix is equivalent to adding up about 10^{30} numbers, which is a task that is classically intractable for non-trivial matrices. More importantly, the scheme we developed can quantify geometric discord in the system [12–15], therefore it allows a systematic study of the computational power of discord. Besides providing an experimental test of the protocol in high-dimensional Hilbert space and ultimately a test of the scalability and resilience of mixed-state computation, this work proposes an application of DQC1 to measure the mean-field interaction strength in a large ensemble of many interacting particles. Finally we provide a general scheme to extend the protocol to different controlled unitaries, such as those encountered in many-body physics, quantum thermodynamics and quantum metrology [16, 17].

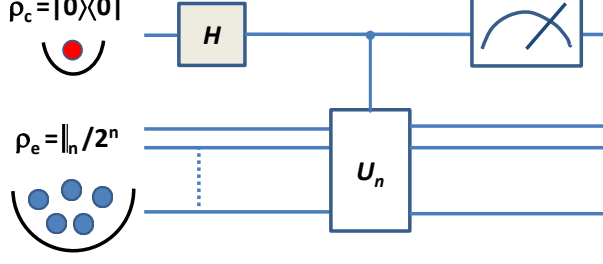


FIG. 1. (Color online). Circuit model of the DQC1 algorithm. The control atom and the ensemble are optically trapped at a distance and individually optically addressed. The control atom is prepared in a pure state $|0\rangle\langle 0|$ whilst the ensemble atoms are prepared in the maximally mixed state.

II. DQC1

Fig. 1 describes the DQC1 algorithm: the input state consists of a single control qubit, whose purity can be varied, prepared in the state $|0\rangle\langle 0|$ and a register of n qubits which are in the maximally mixed state $I_n/2^n$. After a Hadamard operation on the single qubit, a controlled unitary U_n is performed on the n -qubits mixed state.

This has the effect of encoding the normalized trace of the unitary operation into the single qubit coherences, and the output state of the control qubit can be written as:

$$\rho_{C_{out}} = \frac{1}{2} \begin{pmatrix} 1 & \frac{\text{Tr}[U_n^\dagger]}{2^n} \\ \frac{\text{Tr}[U_n]}{2^n} & 1 \end{pmatrix} \quad (1)$$

The trace of the unitary U_n can then be retrieved by measurement of the expectation values of the Pauli operators (X and Y) on the single qubit, as $\langle X \rangle = \text{Re}[\text{Tr}(U_n)]/2^n$ and $\langle Y \rangle = -\text{Im}[\text{Tr}(U_n)]/2^n$.

III. DQC1 WITH ATOMS

In the scheme we propose, the control qubit can be stored either in the ground states of a single atom or in an ensemble of strongly interacting atoms, using techniques that have been recently proposed to prepare and control mesoqubits [18]. For clarity we will refer to the control qubit as a single atom qubit, but an extension of the protocol to a mesoqubit is straightforward. The single atom qubit is used as the control for a unitary operation, enabled by Rydberg-Rydberg interactions, on a register of n qubits encoded in an ensemble of atoms, as shown in Fig. 1.

The control qubit and the ensemble are stored in two separate micron-sized dipole traps that are individually addressable [19] [20]. In the case under study the qubit is encoded in the two ground state hyperfine levels of ^{87}Rb

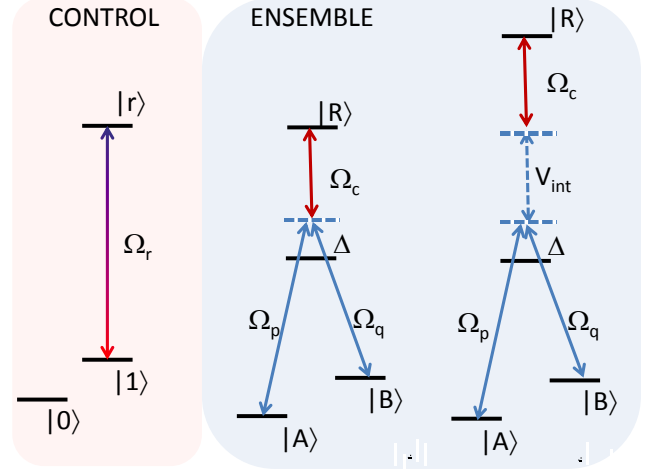


FIG. 2. (Color online). Optical scheme to implement the controlled off-resonant Raman rotation. The control qubit is encoded in the states $|0\rangle$ and $|1\rangle$ of a single atom. State $|1\rangle$ is coupled to a Rydberg state via Ω_r . Each of the n qubits in the ensemble is encoded in the states $|A\rangle$ and $|B\rangle$ which are coupled by a 2-photon scheme similar to [20]. A beam coupling the intermediate state to the Rydberg state is added so that the EIT condition is fulfilled and the interaction with Ω_p and Ω_q is inhibited (left panel). However the coupling of the control atom to Rydberg state can activate an additional shift that removes the condition for EIT, so that off-resonant Raman transfer is activated (far-right panel).

(in Fig. 2 represented by $|0\rangle$ and $|1\rangle$). The ensemble qubits are first encoded in the same hyperfine ground states of ^{87}Rb (in Fig. 2 represented by $|A\rangle$ and $|B\rangle$), and the ensemble is subsequently prepared in a highly mixed state. The single qubit acts as a control atom over the target ensemble via excitation to Rydberg state and we use a laser excitation scheme developed in [20] based on electromagnetically induced transparency (EIT) and shown in Fig. 2.

We performed numerical calculations to study the feasibility of the experimental implementation of the protocol to benchmark this method for a specific choice of the unitary and for different number of atoms in the ensemble.

A. Initialization:

The control qubit is first prepared via optical pumping in state $|1\rangle$. A π -pulse (Hadamard rotation via stimulated Raman transition) is then performed to initialize the qubit in $|+\rangle = \frac{1}{\sqrt{2}}(|0\rangle + |1\rangle)$ (Table I). This can be achieved with a fidelity $> 99.9\%$, as discussed in [21]. The control qubit is therefore prepared in a superposition of states $|0\rangle$ and $|1\rangle$, and, in general, its purity can be varied. Similarly, the ensemble state is obtained by first preparing a 50/50 weighted superposition

	Initialization	Processing		Measure	
C	$ +\rangle = \frac{1}{\sqrt{2}}(0\rangle + 1\rangle)$	Ryd π		Ryd π	X(Y) fluo
E	$I_n/2^n$		CU_n		

TABLE I. Summary of the sequence of operations on the control and ensemble qubits to perform the DQC1 protocol. After the initialization stage the qubit is prepared in $|+\rangle = \frac{1}{\sqrt{2}}(|0\rangle + |1\rangle)$ and the ensemble in a maximally mixed state. The processing stage sandwiches a controlled unitary between two π -pulses (the first couples state $|1\rangle$ to a Rydberg state and the second returns back to the ground state), so that the control qubit acquires some Rydberg character necessary to operate the controlled unitary and it is then returned to its original state. Fluorescence measurements are performed on the populations of states $|0\rangle$ and $|1\rangle$ after an X-(Y) rotation.

$|+\rangle_n = \frac{1}{\sqrt{n}}(|0\rangle + |1\rangle)^{\otimes n}$ by applying the Hadamard gate to the whole ensemble containing n atoms. To introduce the “mixedness” we propose a method adapted from a scheme developed for ions [22]: following the preparation of state $|+\rangle_n$, one of the two ground states is coupled to the intermediate state $|P\rangle$ so that optical pumping exposes the ensemble to decoherence and a mixed state is prepared. We operate the optical pumping over a stretched state, so that there is no loss of population and the mixed state can be prepared with optimum efficiency.

The purity of the control qubit and the mixedness of the ensemble are controlled using the same level scheme described in figure III A

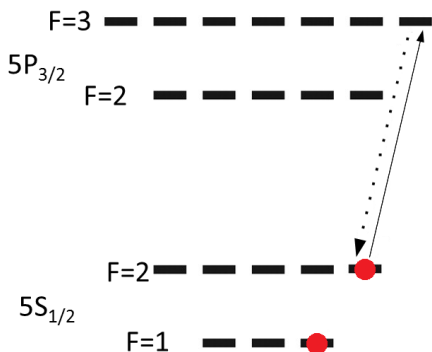


FIG. 3. States $|0\rangle$ and $|1\rangle$ are $5S_{1/2}$, $F = 1$, $m_F = 1$ and $5S_{1/2}$, $F = 2$, $m_F = 2$ respectively. Following the preparation of state $|+\rangle_n$, state $|1\rangle$ is coupled to the intermediate state $5P_{3/2}$, $F = 3$, $M_F = 3$ via σ - polarised light, so that optical pumping exposes the ensemble to decoherence and a mixed state is prepared. This method is used both to prepare the ensemble in a maximally mixed state and to vary the purity of the control qubit.

B. Processing:

The DQC1 protocol relies on a controlled unitary performed on an ensemble of atoms prepared in a highly mixed state. To benchmark the protocol we choose to apply a controlled non-resonant Raman rotation to the ensemble atoms qubits. This is done exploiting a scheme similar to the one developed in [20] for CNOT gates. We find that the protocol, described in Fig. 2, works very efficiently with high fidelity for any controlled-rotations.

The processing stage begins with a π pulse applied to the control atom so that the coupling between state $|1\rangle$ $|r\rangle$ is activated, as shown in the Table I. An off-resonant Raman pulse is then applied to the ensemble atoms to performs rotations of the ensemble qubits corresponding to different angles in the Bloch sphere.

We performed simulations of this scheme by numerically solving the time dependent Schrodinger equation for a 4-level atomic system in the presence of finite Rydberg blockade and taking into account decay from the intermediate state. We find that, for high fidelity operation for both small and large n , the following conditions have to be fulfilled: i) The Raman detuning Δ has to be much larger than the inverse of the decay rate of the intermediate state, to make sure that spontaneous decays is highly suppressed, ii) the lifetime of the Rydberg state chosen for the control atom has to be much larger than the operation time of the controlled Raman and iii) $\Omega_p, \Omega_q \ll \Omega_c$ to ensure that when the control atom is not in the Rydberg state, the EIT condition is met and there is little unwanted coupling of the ensemble atoms to the light. This is in agreement with [20], where this laser scheme was used to perform controlled logic on ensemble atoms.

We choose $|R\rangle = 63S$ and $|r\rangle = 64S$ for Rubidium 87 that, for a separation between the traps of $1.7\mu\text{m}$, provide an interaction strength in excess of 15 GHz. The Raman beams both have Rabi frequency $\Omega_p = \Omega_q = 2\pi \times 70$ MHz and detuning $\Delta = 2\pi \times 1200$ MHz from the intermediate state. Ω_c is chosen to be $2\pi \times 700$ MHz. This coupling Rabi frequency can be obtained with commercially available intermediate power laser sources focused down to waists of tens of micrometers. With these parameters, the EIT-induced blocking of the Raman transfer works with a fidelity of more than 99.8% [20]. We numerically calculate the evolution of the system after a pulsed Raman rotation of different duration (i.e. corresponding to a different angle in the Bloch sphere) and we retrieve the X(Y) expectation values. We find that the real and imaginary part of the trace of the unitary acting on the ensemble of atoms take the form shown in Fig. 4 for different number of atoms in the ensemble. The slight damping in time of the amplitudes of the peaks reflects a dynamical phase shift, extensively discussed in [20].

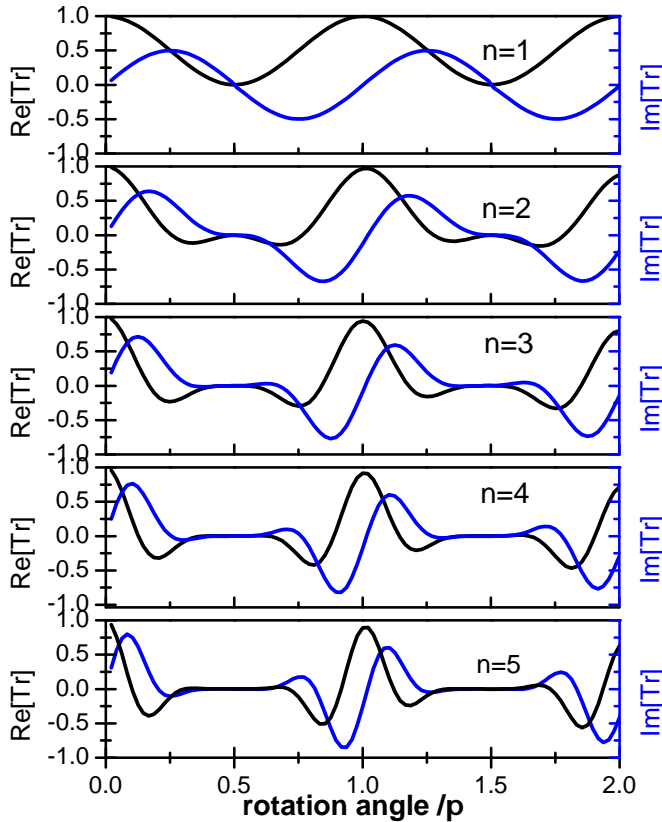


FIG. 4. (Color online). Results of the numerical estimate of the real (black) and imaginary (blue) parts of the normalized trace for $\Omega_p = \Omega_q = 2\pi \times 70$ MHz, $\Delta = 2\pi \times 1200$ MHz from the intermediate state. The decay rate $2\pi \times 6$ MHz from the intermediate state is also taken into account. Ω_c is chosen to be $2\pi \times 700$ MHz. $|R\rangle = 63S$ and $|r\rangle = 64S$ for Rubidium 87 that, for a separation between the traps of $1.7\mu\text{m}$, provide an interaction strength of 15 GHz. We take into account the decay from the intermediate state.

C. Measure of the trace and geometric discord

At the end of the protocol, the measurement of the state of the control qubit will allow us to retrieve the real and imaginary part of the trace of the unitary respectively. This is done by statistical measurements of the populations of $|0\rangle$ and $|1\rangle$ following an X-(Y-)rotation. X-(Y-)rotations can be performed with very high fidelity so that they negligibly affect the fidelity of the measurement result [23]. To measure the expectation value with an accuracy ϵ requires the number of runs to be $NR \sim 1/\epsilon^2$, as shown in [7]. It is important to note that the number of runs necessary for a set accuracy does not depend on the number of qubits in the ensemble. Furthermore, the populations are measured via fluorescence imaging,

that also suffers for limited efficiency and significant error rate, particularly when working with single atoms. In order to achieve better than a 10% accuracy requires averages over 400 runs.

It needs to be pointed out that both the control atom and the ensemble atoms are randomly loaded in small size dipole traps [19]. The trap can be operated in controlled regimes, so that a single atom can be loaded with probability 80% [19, 24] and it is possible to conditionally start the experiment once an atom is loaded. The ensemble is typically loaded with a Poisson-distributed number of atoms around an average value \bar{n} . At small n , we can force the number of atoms in the trap to be exactly n for every run of the experiment by post-selection and retrieve the traces in Fig. 4 with small uncertainties. But whilst this is reasonable at small n , it would reduce the efficiency of the protocol at high n . We find, however, that for high atom number benchmarking and test for discord can be done by locking of the average number of atoms (which can be tuned by parameters such as trap depth and density of the reservoir). We have estimated the uncertainties in the value of the trace measured arising from the fluctuations in atoms number in the ensemble from run to run. We assume a Poissonian distribution of atom number with average number 100, as in Fig. 5. The height of the peaks are found to be insensitive to the atom number for the parameters chosen in this work. However, as shown in Fig. 5, the width of the features detected in the trace narrows with increased atom number, leading to an uncertainty in the value of the trace measured. For an average atom number $\bar{n} = 100$ Poissonian variations from run to run lead to an uncertainty of less than 5% at all points (it is negligible at the peak, it is maximum at the position of fast variation).

Other sources of uncertainties related to Rydberg interactions within the ensemble do not affect significantly the fidelity of the protocol, provided a suitable choice of $\Omega_{p,q,c}$ is made [20].

Finally, the geometric discord can be quantified by simply performing the controlled-unitary twice in a row in the DQC1 implementation [25], and this measure has the same accuracy discussed for the trace estimation.

IV. IMPLEMENTING NON-TRIVIAL UNITARIES

Besides testing the scalability of DQC1 it will be interesting to extend the DQC1 protocol to the implementation of *non-trivial* controlled unitary. In general U can be time-evolution operator of some physical system and the ability to enable control qubits extends the range of operability of the protocol. We therefore identified a scheme for X_a [26] gate on the ensemble that allows us to add the control to a range of unitaries of interest.

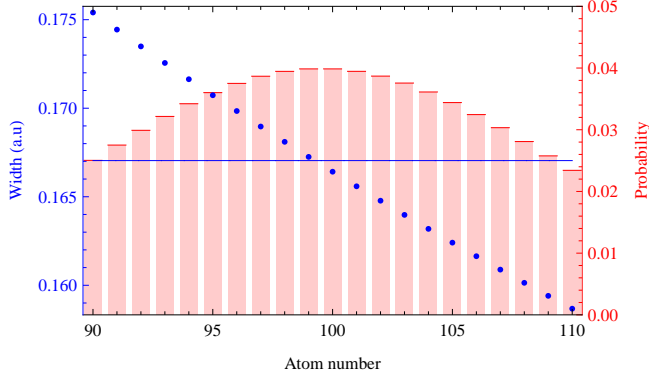


FIG. 5. (Color online). Width of the features in the real part of the normalized trace for different atom number, according to a Poissonian distribution of atom number with average $\bar{n}=100$. Plotted are the probability of loading the trap with a given number of atoms (red) and the width of the peaks in the trace versus atom number (blue). The solid blue line represents the weighted average of the widths, i.e. the result of the measurements.

A. The X_a gate

Any quantum operation (e.g. a unitary evolution) can be made to depend on the state of a control qubit, using the general results presented in Ref. [26]. This work demonstrates the equivalence between a controlled unitary and a sequence of a controlled- X_a gate followed by the quantum operation and the same CX_a gate afterwards, as shown in Fig. 6. This result simplifies the task of finding interesting controlled unitaries that could be implemented in the Rydberg-DQC1 experiment into the task of designing a cold atom version of the controlled- X_a gate.

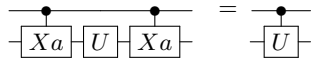


FIG. 6. Circuit identity showing how two controlled- X_a gates can be used to implement an arbitrary unitary, U , in a controlled way.

To explain in more detail, the X_a gate operates on a four-dimensional Hilbert space spanned by the qubit states, $|0\rangle$ and $|1\rangle$, and two auxiliary states, $|2\rangle$ and $|3\rangle$. The auxiliary states are chosen so that they are not acted upon by the quantum operations that act on the qubit states. The truth table for the X_a gate reads:

$$\begin{aligned} X_a|0\rangle &= |2\rangle & X_a|1\rangle &= |3\rangle \\ X_a|2\rangle &= |0\rangle & X_a|3\rangle &= |1\rangle \end{aligned} \quad (2)$$

Here we propose a scheme to perform a controlled

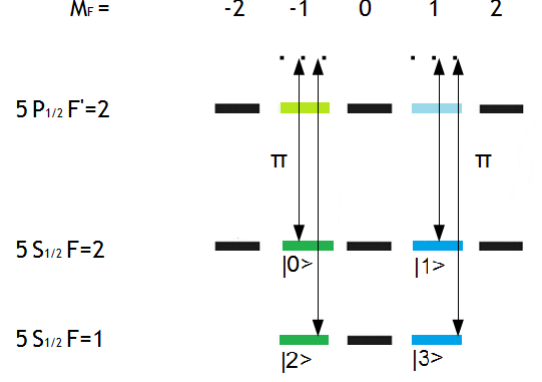


FIG. 7. (Color Online). Transfer between $|0\rangle = |5S_{1/2}, F = 2, m_F = -1\rangle$ and $|2\rangle = |5S_{1/2}, F = 1, m_F = -1\rangle$ (shown in dark green), is provided by a controlled off-resonant Raman transition using linearly polarised light via $5P_{1/2} F' = 2, m_F' = -1$ (shown in light green). Transfer between $|1\rangle = |5S_{1/2}, F = 2, m_F = 1\rangle$ and $|3\rangle = |5S_{1/2}, F = 1, m_F = 1\rangle$ (shown in dark blue), is provided by a controlled off-resonant Raman transition using linearly polarised light via $5P_{1/2} F' = 2, m_F' = 1$ (shown in light blue). When the transfer pulses are π -pulses, an X_a gate is implemented. A controlled- X_a gate can be performed by adding a coupling laser so that EIT occurs conditionally depending on the state of a control atom, using the scheme in 2 and different qubit states. A magnetic field has to be added to lift the degeneracy of the Zeeman states (not represented in figure).

X_a exploiting Rydberg blockaded Raman transitions, where a controlled off-resonant Raman scheme enables the transfer of atoms from the qubit basis to the auxiliary one, conditional on the state of the control qubit. In figure 7 the atomic level and the simplified light diagram is summarized and explained. More details on the complete Raman scheme can be found in [27]. A magnetic field has to be added to lift the degeneracy of the Zeeman states (not represented in figure). Our choice of Zeeman states is governed by the consideration that pairs of states $|F, M_F\rangle$ and $|F+1, -M_F\rangle$ experience the same linear Zeeman shifts (see references [28] [29], [30]).

B. Many-body physics

In the paragraph above we have presented a method to add control to any unitary that operates on a given basis via the X_a gate. The task of finding a range of interesting controlled unitaries that can be implemented using this method is therefore simplified.

The study of the time evolution of many-body interacting systems is certainly one of the key drivers for quantum simulators. The DQC1 protocol with atoms would implement a variety of operations and can be used to explore the physics of interacting system. As an example, by coupling the qubit basis to a Rydberg state we

can switch on *interactions* within the ensemble. Efficient coupling to Rydberg states can be obtained using the schemes described in [31]. The requirement of leaving the auxiliary states unaffected is quite easily met because of the large separation between the hyperfine levels of the ground state (6.8 GHz). It can be shown that, in the regime of strong interactions (i.e. Rydberg-Rydberg interaction strength much larger than Rabi couplings) a measure of the normalised trace of the time-evolution operator at different times will retrieve an average value over the ensemble for the interaction strength.

Finally, this implementation with cold atoms is extremely versatile. The ‘target’ atoms can be arranged in arrays of dipole traps [32, 33] where each site is individually addressable, so that different unitary operations can be performed on different qubits.

This work will motivate the design of protocols to solve a range of problems computationally hard, like finding the ground state of the 2- or 3-dimensional Ising model with a local transverse field with interactions beyond nearest neighbours [34] or studying the unitaries involved in collisions of Rydberg polaritons [35].

V. CONCLUSIONS

We have demonstrated the theoretical feasibility of the implementation of a DQC1 protocol in cold atoms ensemble. The validity of the protocol extends to high n and allows to operate the DQC1 model to compute sums over extremely large strings of numbers, which make the computation classically intractable. Quantum computation has not yet been experimentally studied in large Hilbert spaces, and the successful demonstration of the scalabil-

ity of this protocol would be a major leap forward in the field.

The protocol presented in this work enables us to experimentally test the computational power of quantum discord in a regime never observed so far and it allows a thorough study in high-dimension Hilbert spaces. In particular, by tuning the purity of the control qubit, we can enter regimes with no entanglement and test the efficiency of the algorithm and the power of discord as a resource for quantum computation.

It is important also to point out that non-trivial unitaries can be designed [26] as part of specific algorithms that would allow the implementation of a range of intractable tasks. We have proposed here a general scheme that allows the implementation of a controlled-*many-body* unitary. It is therefore possible to envisage a new tool to explore the physics of many-body interacting systems, by exploiting DQC1 to enable the measurement of the expectation values of operators acting on ensemble of strongly interacting qubits.

Besides providing a unique test for discord, this protocol can also be directly used for quantum phase estimation using large ensembles [2] and as a probe for quantum thermodynamics [16, 17]. The proposed experiment can also be adapted to investigate quantum chaos [36, 37] or to perform the overlap measurement scheme [38], and has the potential to play a role in addressing some fundamental questions like macrorealism [39] and contextuality [40].

This work was supported by EPSRC. The authors thank A. Datta, J. Bolton, K. Modi, H. Cable, C. MacCormick, V. Vedral I. Beterov for helpful discussions and W. Li and I. Lusanovsky for the C_6 coefficients.

-
- [1] K. Modi, A. Brodutch, H. Cable, T. Paterek, and V. Vedral, *Rev. Mod. Phys.* **84**, 1655 (2012).
 - [2] K. Modi, H. Cable, M. Williamson, and V. Vedral, *Phys. Rev. X* **1**, 021022 (2011).
 - [3] B. P. Lanyon, M. Barbieri, M. P. Almeida, and A. G. White, *Phys. Rev. Lett.* **101**, 200501 (2008).
 - [4] M. P. Almeida, F. de Melo, M. Hor-Meyll, A. Salles, S. P. Walborn, P. H. S. Ribeiro, and L. Davidovich, *Science* **316**, 579 (2007), <http://www.sciencemag.org/content/316/5824/579.full.pdf>.
 - [5] T. Werlang, S. Souza, F. F. Fanchini, and C. J. Villas Boas, *Phys. Rev. A* **80**, 024103 (2009).
 - [6] A. Ferraro, L. Aolita, D. Cavalcanti, F. M. Cucchietti, and A. Acin, *Phys. Rev. A* **81**, 052318 (2010).
 - [7] A. Datta, S. T. Flammia, and C. M. Caves, *Phys. Rev. A* **72**, 042316 (2005).
 - [8] A. Datta, A. Shaji, and C. M. Caves, *Phys. Rev. Lett.* **100**, 050502 (2008).
 - [9] A. Datta, *Nature Photonics* **6**, 724 (2012).
 - [10] G. Passante, O. Moussa, C. A. Ryan, and R. Laflamme, *Phys. Rev. Lett.* **103**, 250501 (2009).
 - [11] E. Knill and R. Laflamme, *Phys. Rev. Lett.* **81**, 5672 (1998).
 - [12] B. Dakić, Y. O. Lipp, X. Ma, M. Ringbauer, S. Kropatschek, S. Barz, T. Paterek, V. Vedral, A. Zeilinger, aslav Brukner, and P. Walther, *Nature Physics* **8**, 666 (2012).
 - [13] Y. Yao, H.-W. Li, X.-B. Zou, J.-Z. Huang, C.-M. Zhang, Z.-Q. Yin, W. Chen, G.-C. Guo, and Z.-F. Han, *Phys. Rev. A* **86**, 062310 (2012).
 - [14] ArXiv:1206.4075 [quant-ph].
 - [15] S. Adhikari and S. Banerjee, *Phys. Rev. A* **86**, 062313 (2012).
 - [16] R. Dörner, S. R. Clark, L. Heaney, R. Fazio, J. Goold, and V. Vedral, *Phys. Rev. Lett.* **110**, 230601 (2013).
 - [17] L. Mazzola, G. De Chiara, and M. Paternostro, *Phys. Rev. Lett.* **110**, 230602 (2013).
 - [18] I. I. Beterov, M. Saffman, E. A. Yakshina, V. P. Zhukov, D. B. Tretyakov, V. M. Entin, I. I. Ryabtsev, C. W. Mansell, C. MacCormick, S. Bergamini, and M. P. Fedoruk, ArXiv:1212.1138 [quant-ph].
 - [19] S. Bergamini, B. Darquié, M. Jones, L. Jacubowicz, A. Browaeys, and P. Grangier, *J. Opt. Soc. Am. B* **21**, 1889 (2004).

- [20] M. Müller, I. Lesanovsky, H. Weimer, H. P. Büchler, and P. Zoller, *Phys. Rev. Lett.* **102**, 170502 (2009).
- [21] M. Saffman, X. L. Zhang, A. T. Gill, L. Isenhower, and T. G. Walker, *Journal of Physics: Conference Series* **264**, 012023 (2011).
- [22] J. T. Barreiro, P. Schindler, O. Ghne, T. Monz, M. Chwalla, C. F. Roos, M. Hennrich, and R. Blatt, *Nature Physics* **6**, 943 (2010).
- [23] X. Caillet and C. Simon, *Eur. Phys. J. D* **42**, 341 (2007).
- [24] T. Grnzweig, A. Hilliard, M. McGovern, and M. F. Andersen, *Nature Physics* **6**, 951 (2010).
- [25] G. Passante, O. Moussa, and R. Laflamme, *Phys. Rev. A* **85**, 032325 (2012).
- [26] X.-Q. Zhou, T. C. Ralph, P. Kalasuwan, M. Zhang, A. Peruzzo, B. P. Lanyon, and J. L. O'Brien, *Nature Communications* **2** (2011).
- [27] M. Saffman and T. G. Walker, *Phys. Rev. A* **72**, 022347 (2005).
- [28] M. Saffman and T. G. Walker, *Phys. Rev. A* **72**, 022347 (2005).
- [29] E. Brion, K. M. Imer, and M. Saffman, *Physical Review Letters* **99**, 260501 (2007).
- [30] E. Brion, L. H. Pedersen, M. Saffman, and K. Mølmer, *Phys. Rev. Lett.* **100**, 110506 (2008).
- [31] I. I. Beterov, D. B. Tretyakov, V. M. Entin, E. A. Yakshina, I. I. Ryabtsev, C. MacCormick, and S. Bergamini, *Phys. Rev. A* **84**, 023413 (2011).
- [32] S. Bergamini, *J. Opt. Soc. Am. B* **21**, 1889 (2004).
- [33] M. Piotrowicz, M. Lichtman, K. Maeller, G. Li, S. Zhang, L. Isenhower, and M. Saffman, *Arxiv:1305.6102* (2013).
- [34] F. Barahona, *Journal of Physics A: Mathematical and General* **15**, 3241 (1982).
- [35] J. Stanojevic, V. Parigi, E. Bimbard, A. Ourjoumtsev, P. Pillet, and P. Grangier, *Phys. Rev. A* **86**, 021403 (2012).
- [36] D. Poulin, R. Laflamme, G. J. Milburn, and J. P. Paz, *Phys. Rev. A* **68**, 022302 (2003).
- [37] D. Poulin, R. Blume-Kohout, R. Laflamme, and H. Ollivier, *Phys. Rev. Lett.* **92**, 177906 (2004).
- [38] C.-s. Yu, J. Zhang, and H. Fan, *Phys. Rev. A* **86**, 052317 (2012).
- [39] A. M. Souza, I. S. Oliveira, and R. S. Sarthour, *New Journal of Physics* **13**, 053023 (2011).
- [40] O. Moussa, C. A. Ryan, D. G. Cory, and R. Laflamme, *Phys. Rev. Lett.* **104**, 160501 (2010).